Canadian Journal of Earth Sciences

Article

Ontogeny of *Euphanerops longaevus* from the Upper Devonian Miguasha Fossil–Fish–Lagerstätte and comparison with the skeletogenesis of the sea lamprey *Petromyzon marinus*

Marion Chevrinais[a], **Catherine Morel**[a], **Claude B. Renaud**[b], **and Richard Cloutier**[a]

[a]Laboratoire de Paléontologie et biologie évolutive, Université du Québec à Rimouski, Rimouski, QC G5L 3A1, Canada; [b]Research and Collections, Canadian Museum of Nature, Ottawa, ON K1P 6P4, Canada

Corresponding author: **Marion Chevrinais** (email: mchevrinais.pro@gmail.com)

Abstract

Ontogeny is of paramount importance to understand evolutionary relationships of organisms. However, in the fossil record, early developmental stages are rarely preserved because of their unmineralized skeleton. Here, we describe the ontogeny of the Devonian jawless fish, *Euphanerops longaevus*, based on observations from more than 3500 specimens. The ontogeny of *Euphanerops* is compared with the development of the median fins of the extant jawless fish, the sea lamprey (*Petromyzon marinus*). From a subsample of 216 specimens of *Euphanerops*, we define three ontogenetic stages: larvae (2–38 mm total length (TL), mostly composed of "*Scaumenella mesacanthi*"), juveniles (28–98 mm TL), and adults (≥90 mm TL) based on the degree of skeletal development, chemical and microscopic compositions. Larvae display three cranial plates, a simple branchial apparatus, notochordal elements, and caudal fin supports. In juveniles, we document the development of paired anteroventral, anal, and median dorsal fins. Given how little information is generally available on ostracoderm ontogeny, the growth series of *Euphanerops* provides an unparalleled opportunity to understand the development of early vertebrate characters.

Key words: jawless fish, ontogeny, lamprey, evolution, Palaeozoic

Introduction

The study of the evolutionary history of vertebrates, and especially of jawless vertebrates needs the complementarity of fossil and extant species (Miyashita et al. 2019*a*). Indeed, Palaeozoic jawless fishes are more diversified than extant ones (12 taxonomic groups contra two today (Larouche et al. 2019)). Therefore, a better understanding of the evolutionary history of early vertebrates should be gained by the study of fossil fish in terms of morphology, development, and ecology. Ontogenetic series are rare in the fossil record of vertebrates but when preserved they provide unparalleled evolutionary insights (Cloutier 2010; Delfino and Sánchez-Villagra 2010; Fröbisch et al. 2010; Sánchez-Villagra 2010; Johanson and Trinajstic 2014; Chevrinais et al. 2017).

Systematic assessment of jawless fish of the Miguasha Fossil–Fish–Lagerstätte

Among the fossils from the Upper Devonian Escuminac Formation (Miguasha, Canada), *Euphanerops longaevus* was described as a jawless fish with a dorsal fin and a heterocercal caudal fin (Woodward 1900). The holotype specimen was interpreted upside-down so the identified elements are in fact the anal fin and a hypocercal caudal fin, respectively. Once reinterpreted, the combination of characters indicates that *Euphanerops longaevus* is an anaspid. Subsequently, the assignment of *Euphanerops longaevus* as an anaspid was challenged (Janvier 1981; Forey 1984; Maisey 1986) because of the absence of anaspid synapomorphies such as triradiate branchial spines and chevron-like scales. A second taxon from Miguasha, *Endeiolepis aneri* (Stensiö 1939), was first described as an anaspid species (holotype and its counterpart, Figs. 1B–1D). *Endeiolepis aneri* shows a dorsal fin along the dorsal border of the trunk (documented as absent from *Euphanerops longaevus*), an anal fin with a triangular shape, a caudal fin and paired anteroventral fins, first described as a modified ventrolateral paired fin-fold (Stensiö 1939). A third anaspid-like taxon (new genus and species) from Miguasha, *Legendrelepis parenti* (Fig. 2C), was erected by Arsenault and Janvier (1991). This taxon was described based on differences with *Euphanerops longaevus*: less-developed nonmineralized squamation, differences in scale morphology, the absence of an annular cartilage, its more anteriorly placed anal fin, the possible retention of a small anterior dorsal fin. Later, *Legendrelepis parenti* was recognized as a junior synonym of *Euphanerops longaevus* (Cloutier et al. 1996; Janvier 1996*b*; Janvier and Arsenault 2007).

Fig. 1. (A) Schematic reconstruction of *Euphanerops longaevus* (note that the interpretation of the positions and sizes of skeletal elements and systems is influenced by taphonomic constraints). (B) *Endeiolepis aneri*, holotype SMNH (Swedish Museum of Natural History). (C) 1308 and its counterpart C.1307 C. (from Stensiö 1939, original legends for anatomical elements). (D) *Endeiolepis aneri* almost complete specimen MNHM 01-159. Black arrows point anteriorly. (E) Histograms of the occurrence of adult specimens of anaspid species found in the Escuminac Formation in relation to the lithofacies (from Cloutier et al. 2011). Lithofacies: 1, sandstone; 2, siltstone; 3, laminites; 4, shale. A, absence of the species; P, presence of the species. Black bars correspond to the number of beds for which the species has been found.

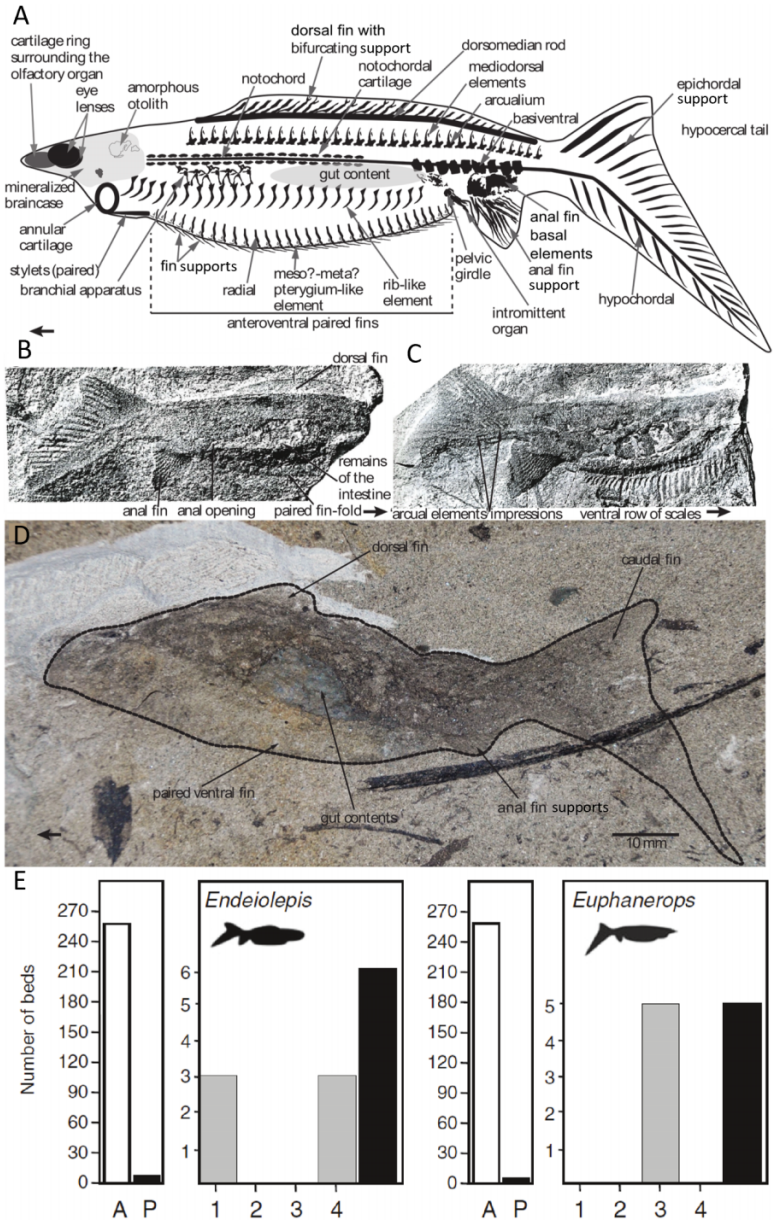

The hypothesis of a synonymy between *Endeiolepis aneri* and *Euphanerops longaevus* also emerges after the analysis of the branchial apparatus of both species suggesting that the observed morphological differences (presence or absence of a dorsal fin, shape of the anal fin) are mainly due to various taphonomical conditions (i.e., preservation in thinly laminated beds, or laminites, for *Euphanerops longaevus* versus sandy turbidite beds for *Endeiolepis aneri*) but the two species remain by absence of definite evidence (Janvier et al. 2006; Janvier and Arsenault 2007). The presence of those species in three types of sediments, sandstone and shale for *Endeiolepis aneri* and laminites for *Euphanerops longaevus* (Fig. 1E) (Cloutier et al. 2011), lead to a difference in the preservation of tissues. Specimens of *Endeiolepis aneri* are mainly preserved as imprints (very poor preservation of mineralized tissues) and sometimes filled with sediments (Figs. 1B–1D), whereas *Euphanerops longaevus* shows 3D preservation and mineralized skeletal elements (Figs. 1A and 2E).

Fig. 2. Photographs and interpretative drawings of *Euphanerops longaevus* of different ontogenetic sizes. (A) NMS 2002.59.17. (B) MHNM 03-1414. (C) MHNM 01-02 A. (D) MHNM 01-150. (E) MHNM 01-123. Large horizontal arrows point anteriorly. Anatomical abbreviations: an. fin support, anal fin support; ann. cart, annular cartilage; arc. L, left side arcualia; arc. R, right side arcualia; a–v fins, anteroventral fins; branchial app, branchial apparatus; d. fin support, dorsal fin support; dmr, dorsomedian rod; epi. support, epichordal support; hypo. support, hypochordal support; int. org, intromittent organ; mm, mineralized matter in the otic region; neuro. el, neurocranial element; no, notochord; pelv. d, pelvic disk. Scale bars: 1 mm (A, B) and 10 mm (C–E). Abbreviations: MHNM, Musée d'Histoire Naturelle de Miguasha, Canada; NMS, National Museums of Scotland, Scotland.

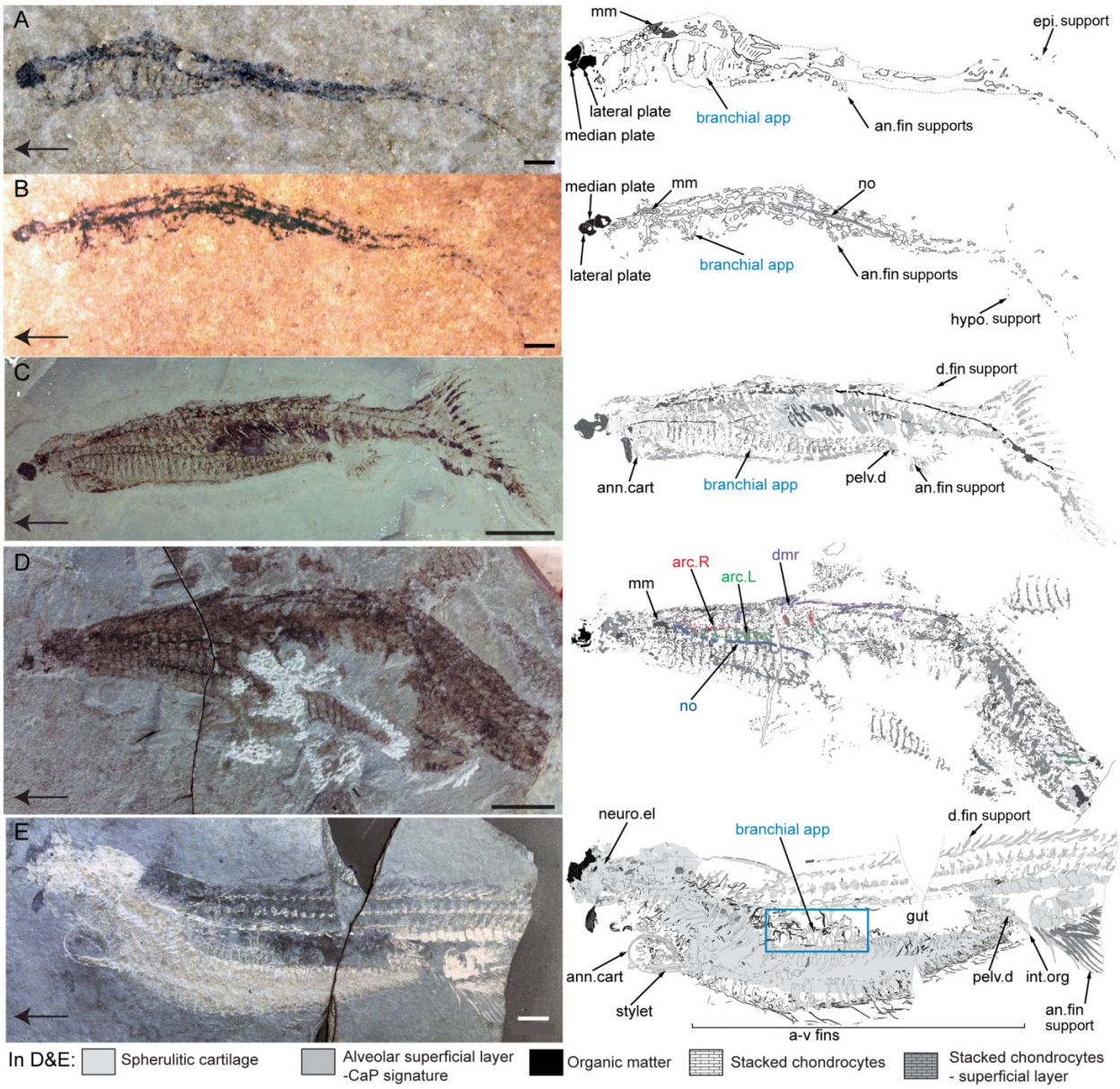

Added to this taphonomic difference, the recent description of the ontogeny of *Euphanerops longaevus* reveals the presence of previously undescribed anatomical elements and especially a dorsal fin extending from the posterior part of the head to anterior to the epicercal lobe of the caudal fin (Figs. 2C and 2E). The dorsal fin is made of a proximal dorsomedian rod and several dorsal fin supports made of stacked chondrocytes. Some dorsal fin supports are bifurcating distally as observed in other jawless fish such as the extant sea lamprey, *Petromyzon marinus*.

Therefore, the differences in taphonomic conditions and the presence of a dorsal fin in *Euphanerops longaevus* as in *Endeiolepis aneri* (Fig. 1) support the latter to be a junior synonym of the former. *Euphanerops longaevus* is thus the only species of "naked" anaspid from the Upper Devonian Escuminac Formation. Finally, the family Euphaneropidae comprises *Euphanerops longaevus* and other "naked" jawless species, *Cornovichthys blaauweni* (Newman and Trewin 2001) and *Achanarella trewini* (Newman 2002) from the Middle Devonian of Scotland (Text S1) (van der Brugghen 2017).

Size series

Only a small subset of specimens has been available to previous authors to reconstruct a growth series of *Euphanerops longaevus*, with the exception of Janvier and Arsenault (2007) who noted immature specimens. In the first half of the 20th century, Graham-Smith (1935) described *Scaumenella mesacanthi* based on 560 specimens from the Upper Devonian Escuminac Formation (Miguasha, Canada) as a "chordate, and probably a vertebrate" because of the presence of a head, a thoracic region with branchial arches, a notochordal or vertebral region, and a hypocercal tail (Fig. 2A, holotype). Until the late 1970s, *Scaumenella mesacanthi* was frequently mentioned when dealing with the origin of vertebrates (Lehman 1957; Tarlo 1960; Piveteau et al.1978) (see Chevrinais et al. 2015*b* for complete literature review). Chevrinais et al. (2015*a*) identified some specimens of *Scaumenella mesacanthi* as early developmental stages of the acanthodian *Triazeugacanthus affinis*, but this taxonomic attribution concerned only 31 specimens. More than 3000 specimens of *Scaumenella mesacanthi* show anatomical characteristics closer to jawless taxa (e.g., *Achanarella trewini*, Newman 2002) than to acanthodians and then could be interpreted as a "naked-anaspid".

The anatomy of *Scaumenella mesacanthi* is poorly known because of the small size of specimens (2–38 mm total length (TL)). Most of the specimens of *Scaumenella mesacanthi* were characterized by a peculiar morphology showing (1) the presence of three head plates (one median and two lateral plates) (Fig. S1), (2) two aggregates of mineralized matter in the otic region (mainly preserved in medium-sized specimens with dorsoventral preservation of the body) (Figs. S1B, S1D, and S1E), (3) a branchial apparatus extending from the head to the anal fin(s), (4) anterior and posterior elements supporting the notochord, and (5) proximal elements of the anal fin(s) (Figs. 2A and 2B). These anatomical elements are absent from specimens of the acanthodian *Triazeugacanthus affinis* in which, however, we observe the presence of three pairs of otoliths, fin spines, and scales.

Numerous beds (horizons) of the Miguasha *Fossil–Lagerstätte* are recognized as a *Konservat-* and *Konzentrat–Lagerstätte* (Cloutier et al. 2011) allowing for the exceptional preservation of unmineralized tissues (carbon signature) indicating weak decay in *Scaumenella mesacanthi* (Fig. 3) (Chevrinais et al. 2015*a*). Thus, the anatomical structures recognized in the specimens of *Scaumenella mesacanthi* were subjected essentially to biomineralization processes and adequately reflect which anatomical elements were preserved at the death of the animal. Based on this peculiar morphology, those specimens of *Scaumenella mesacanthi* are anatomically closer to jawless fishes and especially to Euphaneropidae (Janvier 1996*c*; Janvier and Arsenault 2007) than to the acanthodian *Triazeugacanthus affinis*. In the Musée d'Histoire Naturelle de Miguasha, Canada (MHNM) collection, 2173 specimens from hundreds of plates originally attributed to *Triazeugacanthus affinis* are re-assigned to *Euphanerops longaevus* (Table S1).

Among the two extant clades of jawless fishes, lampreys (Petromyzontiformes) are either considered as the sister-group to living gnathostomes forming the Vertebrata (Bardack and Zangerl 1971; Hardisty 1979, 1982; Janvier 1981; Donoghue and Sansom 2002), the sister-group to hagfishes (Myxiniformes) forming a monophyletic Cyclostomata (Heimberg et al. 2010; Janvier 2010; Miyashita et al. 2019*a*, 2021), or the sister-group to anaspids forming a clade basal to other vertebrates (Chevrinais et al. 2018). Lampreys have many primitive traits of the vertebrate crown, such as neural crest cells (Green and Bronner 2014) and dorsal vertebral elements (arcualia) (Shimeld and Donoghue 2012). However, the homology of numerous skeletal elements between extant agnathans and gnathostomes is unclear because extant cyclostomes have distinct morphology and comparative development reveals few similarities (Miyashita et al. 2019*b*). In lampreys, skeletal development can be followed through life history. Our study is the first to describe the developmental pattern and morphology of the skeletal elements forming the axial (i.e., arcualia) and appendicular (i.e., fin supports) skeletons in the sea lamprey, *Petromyzon marinus*.

Similar to Janvier and Arsenault (2007) who re-described the anatomy of *Euphanerops longaevus* in light of lamprey morphology, Chevrinais et al. (2018) recently described the axial skeleton and the paired appendages of *Euphanerops longaevus.* To complete this description, we focus on ontogeny. Our main objectives are to describe the growth of *Euphanerops longaevus* in comparison with the ontogeny of living lampreys, and to address the homology of the axial and appendicular skeletons in early vertebrates.

Materials and methods

Petromyzon marinus

The sea lamprey *Petromyzon marinus* was sampled from (1) Lake Huron basin (ON, Canada) and the Sainte-Anne River (QC, Canada) (Fish Collection of the Canadian Museum of Nature (CMNFI)), (2) the Old Woman River (ON, Canada) (Bayfield Institute (Fisheries and Oceans Canada)), and (3) the Saint Lawrence River (QC, Canada) (Maurice-Lamontagne Institute (Fisheries and Oceans Canada)). Specimens were cleared and stained following Chevrinais et al. (2018).

To characterize the order of developmental events occurring in the median fins of ammocoetes, generalized linear models were fitted against the binary data set of skeletal development and tested with χ^2 statistic. These logistic regressions describe the relationship between the continuous predictor variable (i.e., TL) and the random component (i.e., developmental states for each element) and provide an estimate of the TL at which half of the specimens possess the developed element (TL_{50}) (adapted from Fischer-Rousseau et al. 2009; Grünbaum et al. 2012). To minimize a potential interpopulational variation, TL_{50} was performed only on the population of Sainte-Anne River ($n = 54$, TL = 19–129 mm).

Euphanerops longaevus

Specimens of *Euphanerops longaevus* come from the middle Frasnian Escuminac Formation (Miguasha, Canada) (Cloutier et al. 1996). Specimens of *Euphanerops longaevus* and *Scaumenella mesacanthi* are accessioned and catalogued in the MHNM (2173 specimens), National Museums of Scotland, Scotland (NMS) (1355 specimens), and the Natural History Museum, London (NHM) (6 specimens). A subsample of 216

Fig. 3. Anatomical structures, scanning electron microscopy (SEM) and energy dispersive X-ray spectrometry (EDX) analyses of *Euphanerops longaevus*. (A) Juvenile specimen of *Scaumenella mesacanthi* MHNM 01-224_1 with (B) SEM of head plates and respective spectrum. (C) Juvenile specimen MHNM 01-257 with (D) SEM of mineralized matter in the otic region and corresponding spectrum. (E) Juvenile specimen MHNM 01-02 A with (F) SEM of annular cartilage and corresponding spectrum. (G) SEM of hypochordal supports of the caudal fin and corresponding spectrum and (H) SEM of anal fin supports and corresponding spectrum. (I) Juvenile specimen NHM P6813 with (J) SEM of branchial elements and corresponding spectrum. (K) SEM of anal fin basal elements and corresponding spectrum and (L) SEM of epichordal supports of the caudal fin and corresponding spectrum. Chemical elements: Al, aluminum; C, carbon; Ca, calcium; F, fluorine; Fe, iron; P, phosphorus; O, oxygen; Si, silicon. Black arrow points anteriorly. Red arrows indicate the EDX position. Scale bars: 5 mm (A, C), 500 μm (B, F, G, K), 10 μm (D), 10 mm (E, I), 100 μm (H), and 50 μm (J, L).

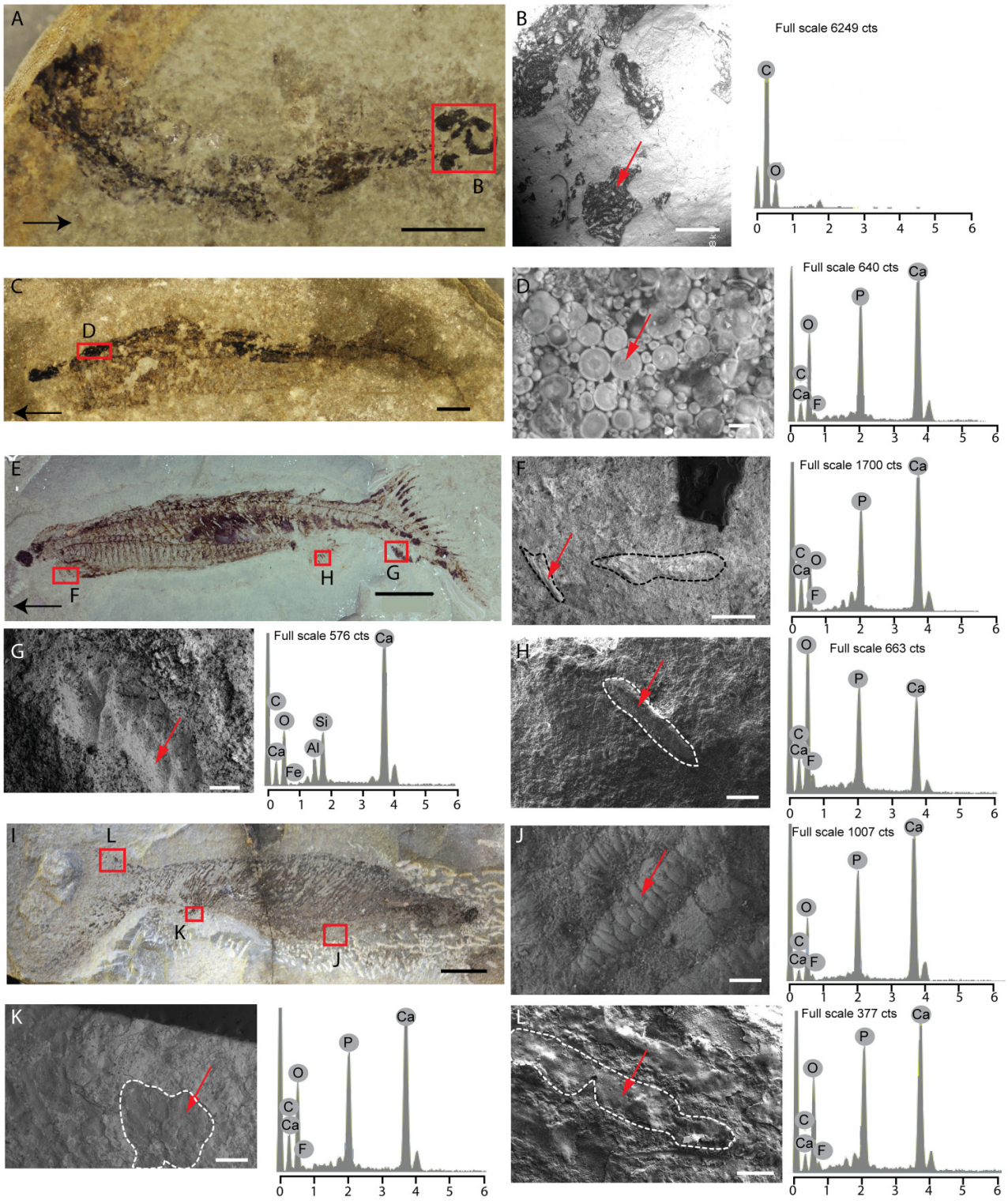

specimens was selected based on (1) diagnostic features of *Euphanerops longaevus* (e.g., three cranial plates, absence of three distinct pairs of otoliths) (Fig. 1), (2) integrity of the specimens (e.g., specimens without preparation artefacts), and (3) presence of representatives along an optimized size range. Specimens have been observed under water immersion (Leica MZ 9.5), drawn using a *camera lucida*, and photographed (Nikon D300). Continuous (length of skeletal elements and distances among them) and discrete data (presence/absence of skeletal structures) were collected (Table S2).

Linear regressions between $\log_{10}$-transformed measurements and TL have been calculated. The developmental trajectory (Grünbaum et al. 2012), defined as the cumulative number of 26 skeletal elements was calculated in relation to TL and estimated TL. A histogram of the distribution of the TL of specimens for each morphotype was constructed. Analyses of variances (ANOVAs) for ratios (median plate length/TL and lateral plate length/TL as a function of morphotypes) were generated using a one-way ANOVA, then pairwise comparisons between groups have been done using a Tukey's test. All statistical analyses have been done with R 3.5.1 (R Core Team 2022).

Elemental composition was analysed and interpreted following Chevrinais et al. (2018).

Results

Skeletogenesis of *Petromyzon marinus*

The development of the neurocranial and branchial skeleton occurs during the prolarval stage in *Petromyzon marinus* (Text S2). In the adult, the branchial basket is composed of seven branchial arches, interconnected dorsally by the subchordal bar and ventrally by the hypobranchial bar (Fig. 4A).

The number, position, shape, and relative proportion of the skeletal elements of the neurocranial, branchial, and axial skeletons remain unchanged for our sampled specimens, ranging from 19 to 129 mm TL. However, the appendicular skeleton (i.e., fin supports) shows progressive development as the size of ammocoetes increases. Based on fin support development, seven developmental steps were identified. Step 1 (Fig. S2A) is defined by the absence of cartilaginous fin supports in the first (D1) and second dorsal (D2) fins (TL < 30 mm). Starting at 31.6 mm TL_{50} (Fig. S3; p value = 1.187e-7), step 2 corresponds to the formation, in the anteriormost region of D2 (Fig. S2B), of the first fin supports (unsegmented, short, and cylindrical cartilaginous rods formed by continuous stacking of flat chondrocytes (Fig. 5A)). Fin supports are not linked to endoskeletal elements; thus, no connection exists between the fin supports and the axial skeleton. In step 3, fin supports develop anteroposteriorly in D2; supports are present at between 75% and 100% of the length of D2 (Fig. S2C). No fin supports were detected in other fins at this step. In step 4, fin supports start to form bidirectionally in the epichordal and hypochordal lobes at the posteriormost region of the caudal fin (TL_{50} = 34.4 mm, p value = 1.691e-10); simultaneously, fin supports appear in the anteriormost region of D1 (Fig. S2D). In step 5, well-developed supports in all three fins (Fig. S2E) indicate the completion of the development. In step 6, fin supports of the caudal fin are longer and dichotomously branched (Fig. S2F); however, this latter condition is not observed in every fin support, even in the later developmental step. In step 7, bifurcation is present in D2 (TL_{50} = 67.6 mm, p value = 2.854e-11) and subsequently in D1 (TL_{50} = 115.9 mm, p value = 0.001). During this step, second-order bifurcation appears in both lobes of the caudal fin (TL_{50} = 100.3 mm, p value = 0.001); new branching is formed symmetrically or asymmetrically on the existing bifurcation of the fin support. Second-order bifurcation appears first in the epichordal and hypochordal lobes, and is occasionally observed in D2 in longer specimens (Fig. 5A). Anterior extension of fin supports in the epichordal lobe is spatially constrained by the presence of D2; the hypochordal lobe is longer than the epichordal lobe and therefore contains more fin supports.

The development of fin supports is positively correlated with the length of ammocoetes as suggested by the results from TL_{50} (Fig. S3). Fin supports develop following a general sequence: fin supports form from anterior to posterior in D2 and in D1, while they form bidirectionally in both the epichordal and hypochordal lobes of the caudal fin. Subsequent skeletal events (i.e., bifurcation and proximal fusion of fin supports) appear as ammocoetes length increases.

The dorsomedian rod is located dorsally to the neural tube (Figs. S4A and S4C). Central chondrocytes are globular and visibly larger than those at the periphery. Groupings of chondrocytes with a similar cellular morphology are present bilaterally on the dorsal part of the notochord (Figs. S4A and S4D), revealing the presence of cartilaginous elements that were not observed on cleared and stained specimens. These elements were found only in the posteriormost region of the caudal fin, attached to the elastic layer of the notochord.

The ventromedian rod lies ventral to the notochord and is formed by a random stacking of globular cells (Figs. S4E and S4F). This rod is at least two to three times higher than the dorsomedian rod. Chondrocytes located ventrally are noticeably different from those in the center. These cells represent the proximal extremity of the fin support, anchored in the ventromedian rod. Increase in shape and size is visible among the cells, as well as the delimitation between cells of the ventromedian rod and the base of the fin support (Figs. S4E–S4G).

Fin supports and branchial arches are similar at both macro- and microscopic levels (Figs. 3E and 4A), and composed of the same type of chondrocytes (closely stacked and elongated with very little ECM) (Figs. S4 and S5). However, the stacking and the shape of chondrocytes in the branchial arches are slightly more regular between rows (Fig. 4E). In fin supports, chondrocytes show various sizes and shapes with largest chondrocytes being at the periphery (Fig. 5A).

Size series and skeletogenesis of *Euphanerops longaevus*

The size series is composed of 216 specimens of *Euphanerops longaevus* ranging from 2 to 278 mm TL (Fig. 6D) including previously described *Euphanerops longaevus* and most of *Scaumenella mesacanthi*. Of the specimens identified distinctly as *Euphanerops longaevus*, three morphotypes are recognized

Fig. 4. Annular cartilage and branchial apparatus in *Petromyzon marinus* and *Euphanerops longaevus*. (A) Adult skeleton of *Petromyzon marinus* (S4-1, 114.1 mm TL), apical cartilages not shown since not visible. (B) Adult specimen *Euphanerops longaevus* MHNM 01-123. (C) Head skeleton of juvenile specimen of *Euphanerops longaevus* MHNM 01-213. (D) Head skeleton of adult specimen of *Euphanerops longaevus* MHNM 01-123. (E) Stacking of chondrocytes in mid-section of branchial arch 7 of ammocoete of *Petromyzon marinus* (CMNFI 2013-0017-S1-41, 75.2 mm TL). (F) Developing cartilaginous protuberances during metamorphosis of *Petromyzon marinus*, branchial arches 6 and 7 of a stage-5 ammocoete (S3-13, 142.9 mm TL). (G) Adult *Euphanerops longaevus* MHNM 01-135 three-sized branchial elements. (H) Adult *Euphanerops longaevus* MHNM 01-123 branchial skeleton. Anatomical abbreviations: a, arcualia; ad, anterior dorsal; al, anterior lateral; ann.cart, annular cartilage; ba, branchial arch; br, branchial ring; co, copula; eh, extra hyal; ep, epitrematic bar; eppr, epitrematic protuberance; hy, hypotrematic bar; hyb, hypobranchial bar; hypr, hypotrematic protuberance; inpr, inferior process; lw, lateral wall of the neurocranium; mde, mediodorsal element; n, notochord; nc, nasal capsule; oc, otic capsule; p, piston; pa, parachordal; pd, posterior dorsal; per, pericardial cartilage; pl, posterior lateral plate; soa, subocular arch; soap, pillar of the subocular arch; st, stylet; sub, subchordal bar; supr, superior process; tr, trabecula; va, velar arch; vp, velar plate. Large horizontal arrows point anteriorly. Scale bars: 5 mm (A), 3 mm (B–D), 0.1 mm (E), and 1 mm (F).

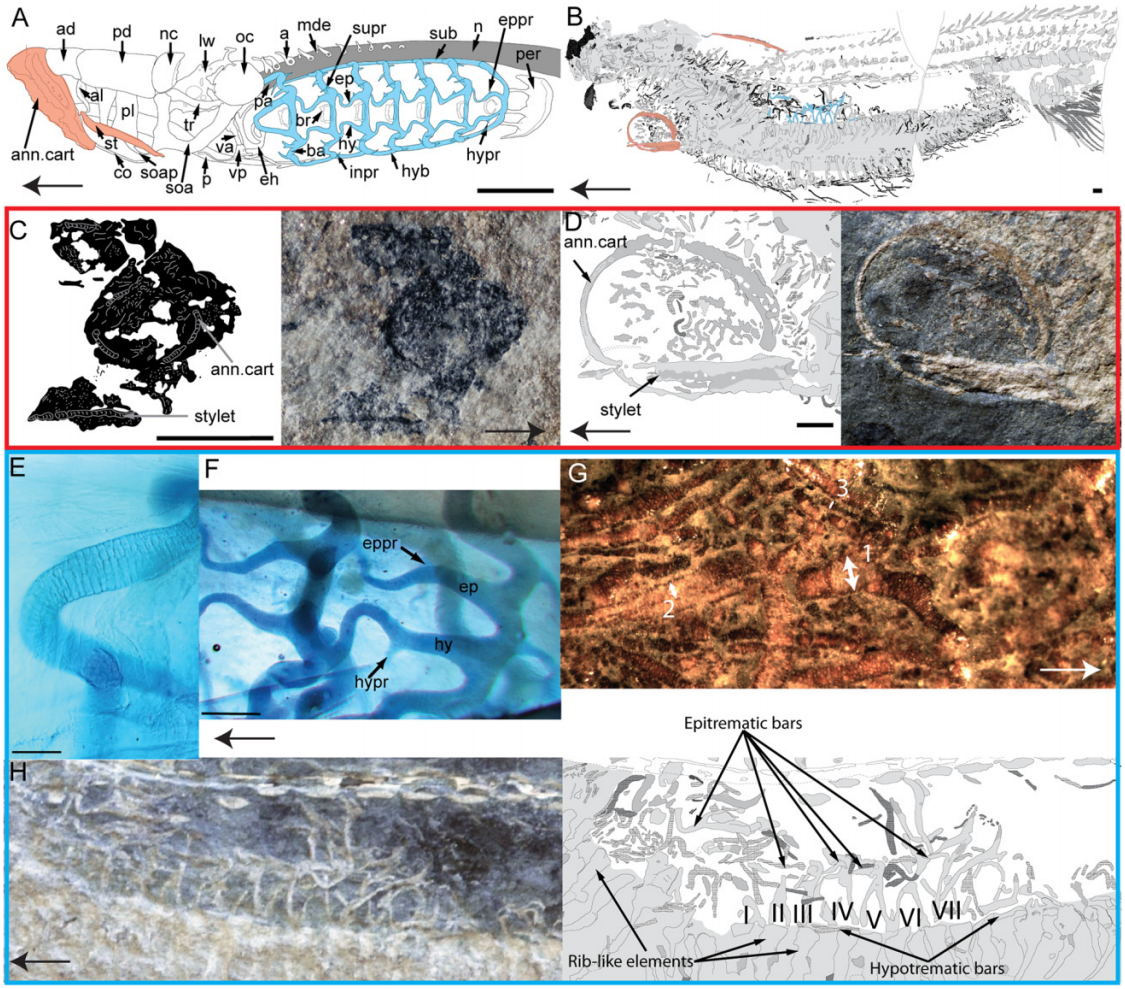

based on (1) presence/absence of skeletal elements (Fig. 7 and Table S2), (2) structure of the developmental trajectory with alternation of thresholds (i.e., periods of numerous additions of skeletal elements) and stases (i.e., periods of few additions of skeletal elements) (Fig. 7), and (3) lengths of skeletal elements relative to TL (Fig. 6C).

The developmental trajectory of *Euphanerops longaevus* shows a main threshold at the beginning of the size series (around 10 mm TL), with the addition of numerous skeletal elements followed by a stasis (between 40 and 90 mm TL); a second threshold is present between 90 and 100 mm TL, showing the transition between morphotypes 2 and 3 followed by a stasis between 100 and up to 278 mm TL (Fig. 7). Morphotype 1 is defined by the numerous addition of anatomical elements associated with TL increase (i.e., 19 neurocranial, branchial, and axial elements out of 26 elements) (Fig. 7). Morphotype 2 is characterized by the stasis of few anatomical changes (Fig. 7). Morphotype 3 is characterized by the addition of few anatomical changes (Fig. 7), a complex branchial skeleton

Fig. 5. Dorsal fin in *Petromyzon marinus* and dorsal and anal fins in *Euphanerops longaevus*. (A) Second-order bifurcation in the second dorsal fin of ammocoete of *Petromyzon marinus* (CMNFI 2013-0019-S2-02, 103.4 mm TL) and detailed morphology of stacked chondrocytes in a dorsal fin support. (B) *Euphanerops longaevus* MHNM 01-123 and details of the dorsal fin (purple), the anal fin(s) (yellow), and the cartilaginous background with spherulitic cartilage (orange). (C) *Euphanerops longaevus* MHNM 01-150 and details of the dorsal fin (purple) and the anal fin(s) (yellow). (D) Anal fin of immature *Euphanerops longaevus* MHNM 01-02 A. Anatomical abbreviations: an.fin support, anal fin support; d.fin support, dorsal fin support; dmr, dorsomedian rod; no, notochord; nt, neural tube. Red asterisks indicate fin supports with first-order bifurcation whereas black ones are for second-order bifurcation. Scale bars: (A) 0.1 mm, (B, D) 3 mm, except the orange rectangle in (B) 1 mm, and (C) 10 mm.

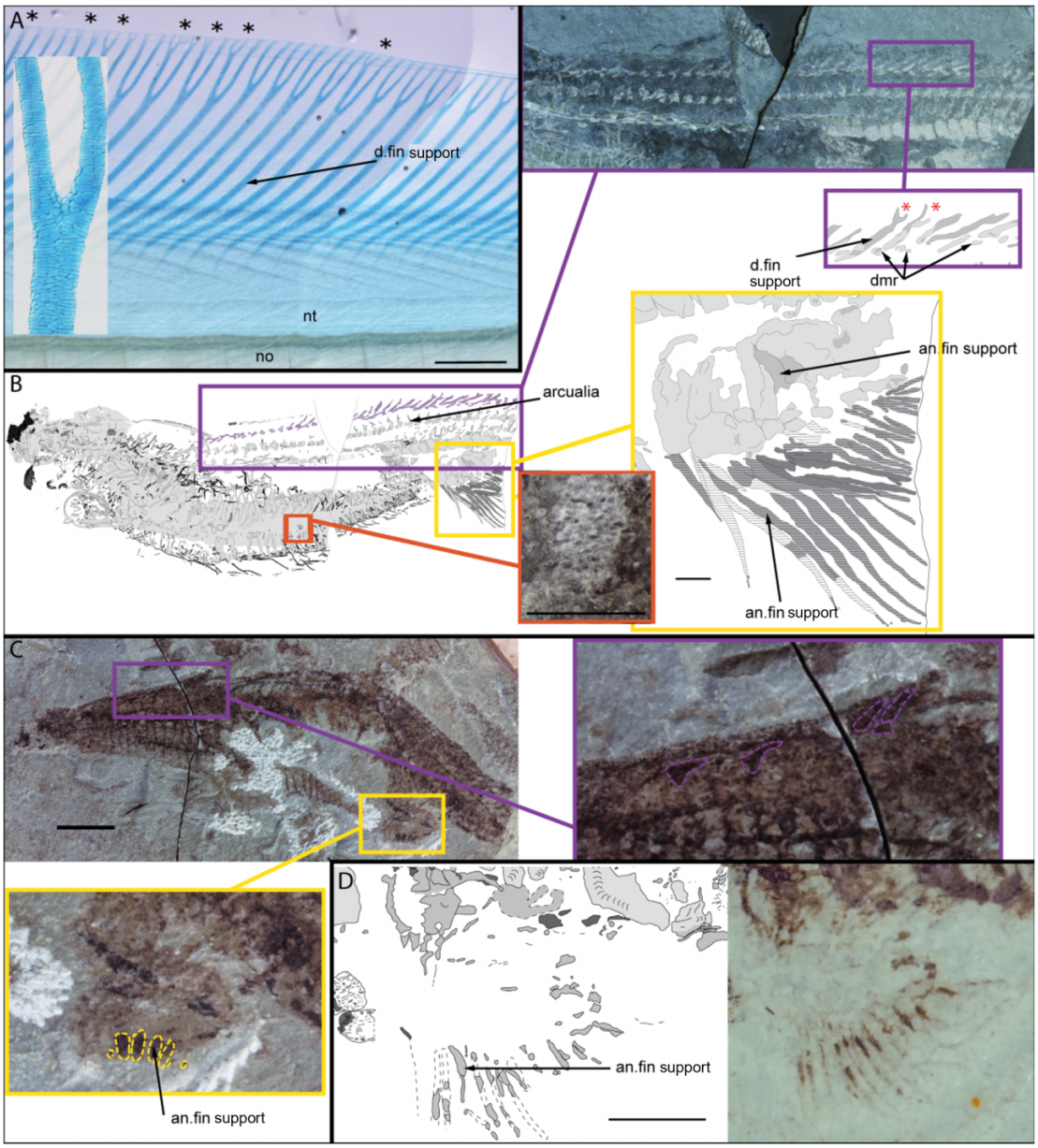

and the completion of mineralization. Various orientations of the body at burial have been observed: morphotype 1 shows small specimens mostly preserved in lateral position (Figs. 2A and 2B), morphotype 2 shows specimens mainly preserved in dorsoventral position (Fig. S1), and morphotype 3 shows larger specimens primarily preserved in lateral position (Figs. 2C–2E).

There is a significant positive linear relationship between the length of the head lateral plate and TL ($n = 129$, $R^2 = 0.88$, p value <2.2e-16, slope: 0.92) and the length of the branchial basket and TL ($n = 99$, $R^2 = 0.81$, p value <2.2e-16, slope: 0.98) (Figs. 6A and 6B). Analyses of variance of (1) head median plate length/TL and (2) head lateral plate length/TL as a function of morphotypes show that there are significant differences between the morphotypes in (1) median plate length/TL (ANOVA, p value = 1.53e-7), but no significant differences in (2) lateral plate length/TL (ANOVA, p value = 0.1319). Furthermore, pairwise comparisons of median plate length/TL

Fig. 6. (A) Relationship between lateral plate length and TL. (B) Relationship between the branchial basket length and TL. (C) Relationship between the ratio of median plate or lateral plates length and the TL in the three morphotypes. (D) Distribution of the three morphotypes (ontogenetic stages) of *Euphanerops longaevus* according to the TL.

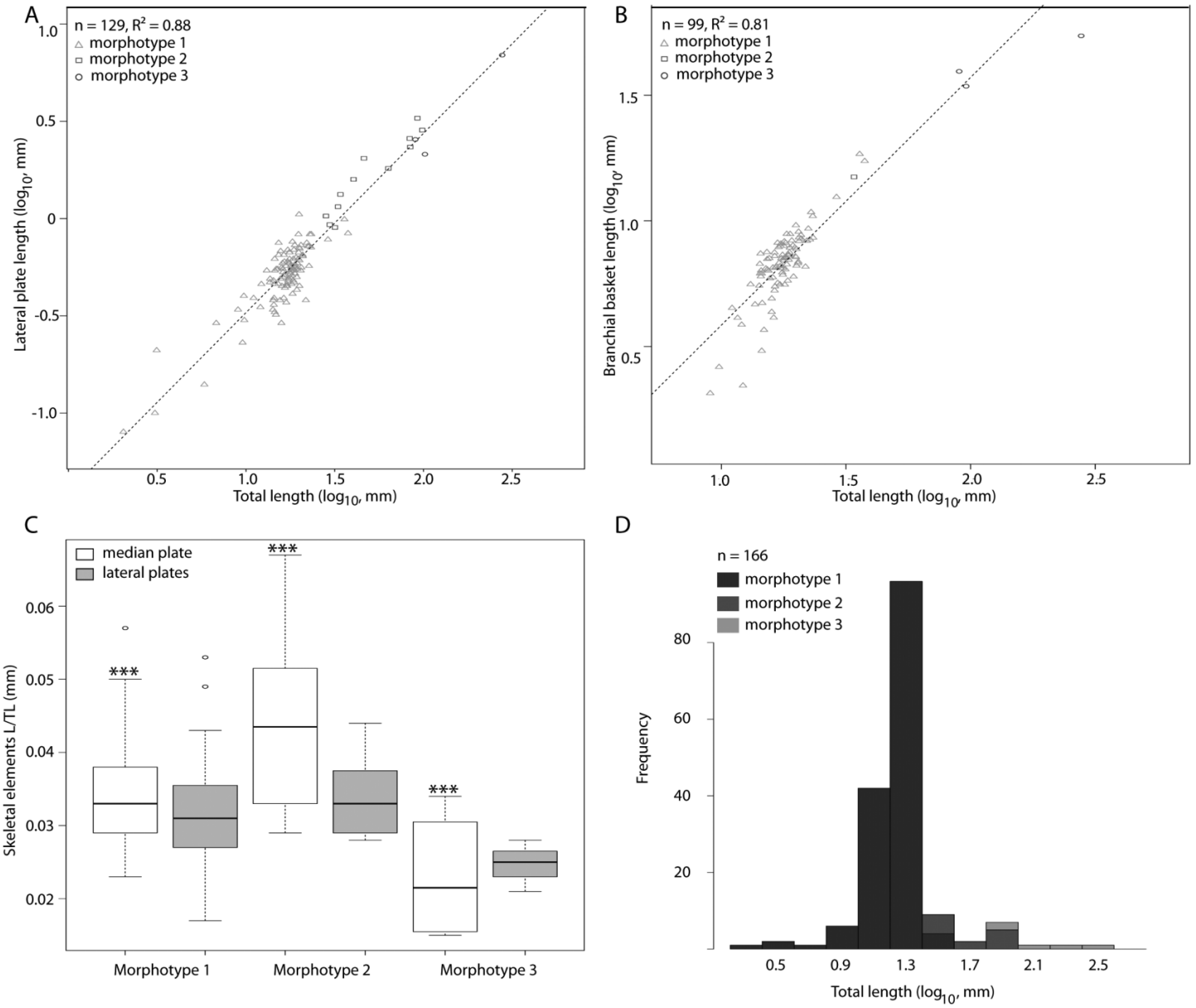

between morphotypes show significant differences in each pair (morphotypes 2–3: p value <0.0001; morphotypes 3–1: p value = 0.006; morphotypes 2–1: p value <0.0001) (Fig. 6C). However, we must consider that the TL of specimens of each morphotype increases progressively although there are some overlaps among morphotypes (Fig. 6D).

The three morphotypes are best interpreted as three ontogenetic stages because of (1) the size of individual skeletal elements (Figs. 6A and 6B), (2) the increase in the number of skeletal elements with TL (Fig. 7), (3) the significant differences in the lengths of skeletal elements among morphotypes (Fig. 6C), and (4) the distribution of morphotypes along the size series (Fig. 6D). Morphotype 1 showing the early development corresponds to the larval stage (166 specimens), morphotype 2 showing a step in the developmental trajectory corresponds to the juvenile stage (30 specimens), and morphotype 3 showing the completion of the mineralization and sexual organs (i.e., intromittent organs) corresponds to the adult stage (20 specimens).

Larvae (2–38 mm TL)

The first developmental stage available for *Euphanerops longaevus* is the larval period; no embryonic specimens have been identified yet (as defined by Cloutier 2010). The general body shape is filiform. In the smallest specimen (2 mm TL, MHNM 01-269), the carbonaceous paired lateral plates and median plate (carbon: 66.3% wt, Figs. 3A and 3B), the

Fig. 7. Developmental trajectory (upper part) and sequence (lower part) of *Euphanerops longaevus*. Light grey background, immature specimens preserved in dorsoventral position; horizontal dashed lines, putative presence of a structure; full boxes, presence of a mineralized structure. Arrows indicate thresholds.

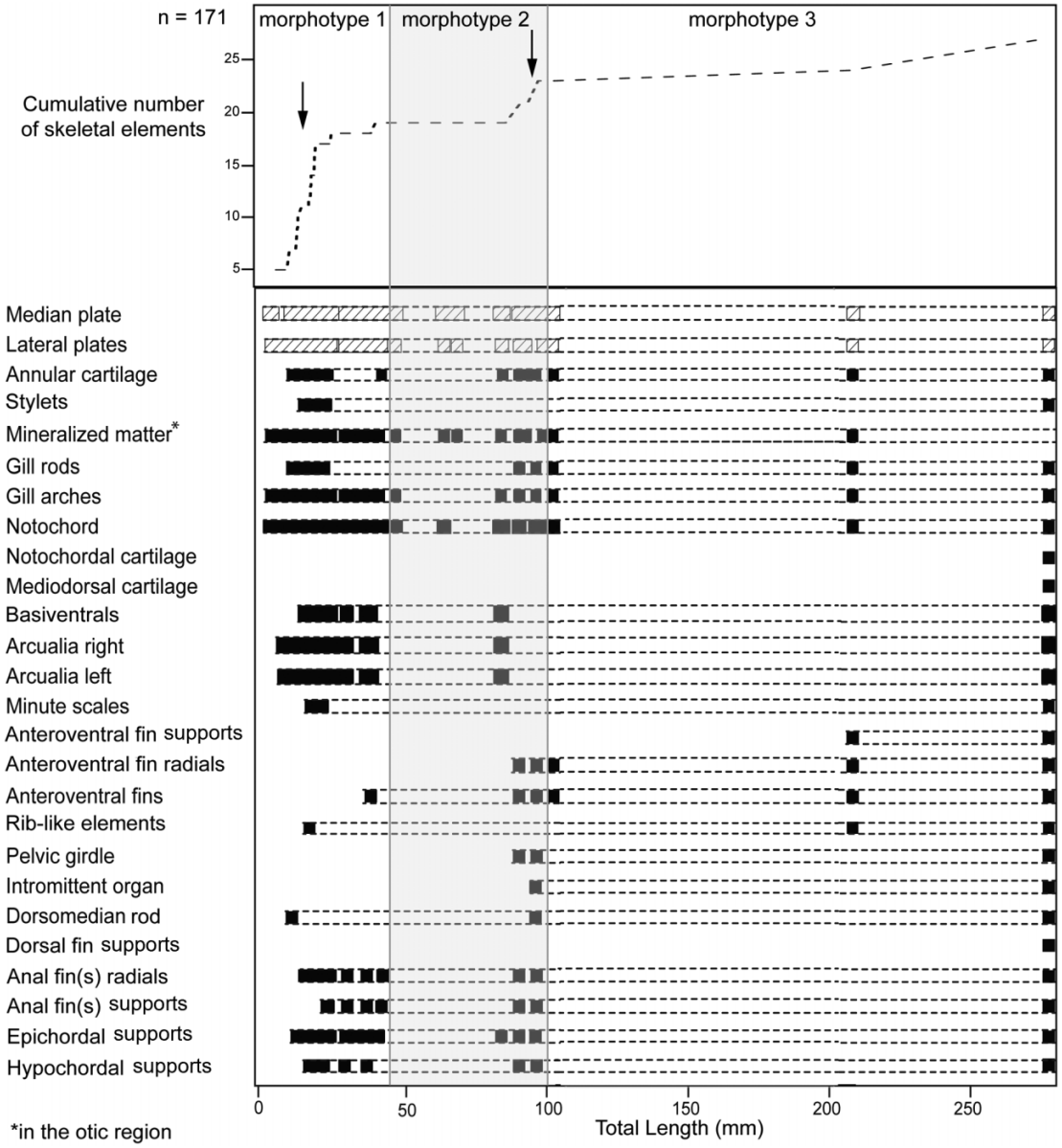

two aggregates of mineralized matter in the otic region, gill arches, and notochordal elements are already developed (Fig. 7). The two aggregates of mineralized matter in the otic region are composed of spherules of various diameters and show several layers (calcium: 24.7% wt, phosphorus: 11.3% wt, fluorine: 5.5% wt, Figs. 3C and 3D). Elements of the vertebral column, left and right arculia are present in specimens as small as 6.8 mm TL (MHNM 01-224_3), followed by the development of the epichordal lobe supports of the caudal fin then the hypochordal lobe supports (11 mm TL (MHNM 01-251) and 15.7 mm TL (MHNM 01-265), respectively). At 9.6 mm TL (MHNM 01-224_2), the dorsomedian rod and the gill rods developed, followed by the annular cartilage and stylets (9.8 mm TL (MHNM 01-244_14) and 13.7 mm TL (MHNM 01-243)). The anal fin radials (14.4 mm TL, MHNM 01-227), basiventrals (14.5 mm TL, MHNM 01-237), rib-like elements (i.e., black longitudinal elements below and perpendicular to the notochord at the level where we found ribs in adults) (15.8 mm TL, MHNM 01-239), and anal fin supports (21.8 mm TL, MHNM 01-230) developed subsequently. Lastly, anteroventral fins are observed as phantom imprints at 37.6 mm TL (MHNM 01-295) (Fig. 7).

Juveniles (28–98 mm TL)

A pattern is recognizable in most specimens where the median plate is larger than the lateral cone-shaped elements (Fig. 6C). The mineralized matter in the otic region is often preserved. The mineralisation of skeletal elements (calcium and phosphorus) such as the supports of the epichordal lobe

(Fig. 3L), gill rods with stacked chondrocytes (Fig. 3J), the annular cartilage (Figs. 3C and 3F), and anal fin radials and supports (Figs. 3H–3K) are observed at this stage. The annular cartilage is present as low relief overlaid by the median plate, the stylets are also observed in relief overlaid by the lateral plates in a dorsoventrally preserved specimen (MHNM 01-213, Fig. 4C). Anteroventral radials and pelvic girdle are recorded at 90 mm TL (MHNM 01-02 A) followed by the presence of intromittent organs at 98 mm TL (NHM P6813) (Chevrinais et al. (2018). The dorsoventral orientation at burial of the body of most juveniles does not allow for an exhaustive anatomical study of the specimens (Fig. S1).

Adults (90–278 mm TL)

The adult stage is characterized by the presence of anatomical structures such as the anteroventral fin supports (208 mm TL, MHNM 01-317), the mediodorsal and notochordal cartilages (Chevrinais et al. 2018), and the late development of dorsal fin supports (278 mm TL, MHNM 01-123) (Fig. 7). In the larger and best-preserved specimen of *Euphanerops longaevus* (MHNM 01-123), the annular cartilage and the stylets are also observed, even if the right-side stylet is displaced and artificially looks like a dorsal spine (Figs. 2E and 4B–4D). At this stage, a modification of the branchial apparatus is also observed (Fig. 4G) showing the presence of skeletal elements of three diameters (likely the epitrematic and hypotrematic bars and protuberances) resembling those from the branchial apparatus of *Petromyzon marinus* (Figs. 4E and 4F) in terms of cellular composition and anatomical structure (Martin et al. 2009). Epitrematic and hypotrematic bars are identified in MHNM 01-123; these are associated with seven arches of the branchial apparatus (Fig. 4H). In MHNM 01-123, we identify repeated elements below the branchial apparatus. These elements have large chondrocyte vacuoles and are herein interpreted as rib-like elements (Fig. 4H). The rib-like elements are lying on a cartilaginous background (in grey in Figs 2E and 3H, and in the orange rectangle in Fig. 5B).

In *Euphanerops longaevus*, the order of fin formation (and largely of appendicular skeletal elements) during development is as follows: (1) caudal fin (epichordal before hypochordal), (2) "paired" anal fin(s), (3) paired anteroventral fins (radials before supports), and (4) dorsal fin (supports before fusion of the dorsomedian rod elements and distal bifurcation) (Fig. 7).

Discussion

Our study has improved upon the pioneering works on the lamprey median fins of Dohrn (1886) and Tretjakoff (1926). Dorhn (1886) illustrated Flossenstrahlen (= fin rays) supporting a dorsal fin in a lamprey ammocoete. Our study describes developmental events in the median fins at the specific stage of ammocoete of the life history of *Petromyzon marinus*. New information on the ontogeny of *Euphanerops longaevus*, and the comparison with the ontogeny of *Petromyzon marinus*, allows us to better identify some skeletal elements (otoliths, branchial apparatus, fins) and provide a background for the study of early vertebrate evolution.

In the growth series of *Euphanerops longaevus* we note a low abundance of specimens between 100 and 200 mm TL (Figs. 6 and 7). This gap is observed because the specimens in this size range are often incomplete. Larval specimens are found in the intertidal (slikke) siltstones and argillites ("laminites" facies), whereas adult specimens are mostly found in sandstone, shale, and laminites (Cloutier et al. 2011). The sediments indicate that the environment at the burial of large specimens was more energetic than the environment at the burial of small specimens allowing the disarticulation and decomposition of skeletons especially of poorly mineralized species. The latest paleoenvironmental study on the Escuminac Formation explains that the anaspids have the lowest fossilisation potential because of their poorly ossified nature; they represent <0.5% of the total relative abundance of specimens (Cloutier et al. 2011). Given that more than 95% of larval specimens of *Euphanerops longaevus* were initially identified as *Scaumenella mesacanthi*, their preservation in laminites is rather exceptional. Therefore, the low number of fossilized adults of *Euphanerops longaevus* reflects true absence of adults in the ecosystem, suggesting that the deposits with adult *Euphanerops longaevus* are allochthonous. The Escuminac paleoestuary was probably a nursery for *Euphanerops longaevus* where larvae were much more abundant than adults.

The cellular and chemical composition of the skeleton of the Devonian *Euphanerops longaevus* recalls the structure of the cartilage observed in the extant *Petromyzon marinus*. However, the Alcian blue stains the collagenous ECM in the lamprey while in *Euphanerops longaevus*, the cellular composition is at least partially made of phosphorus and calcium, suggesting the presence of a perichondrial mineralization when phosphorus and calcium are observed in periphery of the structure (Fig. 3) (Berio et al. 2021) or as suggested by Janvier and Arsenault (2007), the presence of spherules of calcium phosphate in the mineralized interterritorial matrix of cartilage (e.g., rib-like elements, mineralized matter in the otic region). Some elements lack (1) phosphorus and then are likely made of calcified cartilage (e.g., hypochordal lobe supports) or (2) lack both calcium and phosphorus and are likely made of collagenous fibers only (e.g., median and lateral plates). Based on our new ontogenetic observations on *Euphanerops longaevus*, we identify seven of these enigmatic structures observed by Janvier and Arsenault (2007) (Table 1).

Head skeleton

The recording of globular calcified cartilage in the anterior part of the body (Fig. 2E, neuro. el) is characteristic of the presence of a neurocranium but the poor preservation of the shape of this element in *Euphanerops longaevus* does not allow clear interpretation and reconstruction.

In the anteriormost part of the body, the presence of a median plate has already been interpreted as an unpaired sensory organ and likely the nasal sac (Janvier and Arsenault 2007; van der Brugghen 2017). This character is shared with other agnathans, like *Jamoytius kerwoodi*. In that taxon, however, an alternative interpretation is the annular cartilage (Ritchie 1968). In *Euphanerops longaevus*, both the annular cartilage and the median plate are observed

Table 1. Comparison between Janvier and Arsenault (2007) interpretation and the new interpretation concerning the anatomy of *Euphanerops longaevus*.

Arsenault and Janvier (2007)	Chevrinais et al. (2018)	This study
White line	Notochord	Notochord
Doughnut-shaped structure		Semicircular canals because of the association with the otoliths
"Myomeres"		
Black line		
"Skin imprints"		
"Scales"		
Mineralized matter in the otic region		Otoliths
"Diffuse mineralized matter"		Stylets associated with the annular cartilage
Ventral arcualia	Left and right arcualia	
"Posterior haemal series"	Haemal elements	
Anterior haemal series	Notochordal cartilages	
Possible pericardiac cartilage and "diffuse mineralized matter"	Pelvic disks and intromittent organs	
"Intermuscular elements"		Branchial apparatus
"Median stain"		Cartilaginous layer external to the olfactory organ
"Lateral stains", traces of cartilaginous plates protecting the snout or paired eyes		Eye lenses
Dorsal arcualia		Dorsal fin supports and dorsomedian rod

Note: Empty cells are for "not re-interpreted".

simultaneously in 48 specimens (Table S2); therefore, we propose that the median plate corresponds to the layer located externally to the epithelium of the olfactory organ as in *Petromyzon marinus* (Green et al. 2017). The nasal capsule is also present in *Petromyzon marinus*, but it is posteriorly located in the neurocranium in comparison to *Euphanerops longaevus*. Therefore, our interpretation in *Euphanerops longaevus* is based on the median position of this element and the homology in terms of chemical composition (essentially carbon) with the solid semicircular ring of cartilage surrounding the olfactory mucosa of *Petromyzon marinus* (Van Denbossche et al. 1997).

Lateral to the ring of cartilage surrounding the olfactory organ are the paired carbonaceous lateral plates (Figs. 2, 3A, and 3B) in *Euphanerops longaevus*. Janvier and Arsenault (2007) interpreted these lateral plates as traces of cartilaginous plates protecting the snout or paired eyes. Among Escuminac species, eye lenses have also been observed in juvenile *Homalacanthus concinnus* (Gagnier 1996), juvenile *Triazeugacanthus affinis* (Chevrinais et al. 2017), juvenile *Miguashaia bureaui* (fig. 7 in Cloutier 1996), juvenile *Eusthenopteron foordi* (fig. 3 in Schultze 1984), and in juvenile *Quebecius quebecensis* (R. Cloutier, personal observation). In other agnathans, these lateral plates are also found and are interpreted as paired eye stains in *Jamoytius kerwoodi* (Ritchie 1968) and optic capsules in Scottish euphaneropids (van der Brugghen 2017). In the Devonian lamprey *Priscomyzon*, eye lenses are also observed (Miyashita et al. 2021). The presence of melanin has been described in some fossil fish (Grogan and Lund 2000; Lindgren et al. 2012) but scanning electron microscopic images of *Euphanerops longaevus* lateral plates do not reveal the presence of spherulitic elements interpreted as melanosomes (Gabbott et al. 2016). In the extant lamprey *Ichthyomyzon unicuspis*, eye lenses have a cone-shaped posterior morphology when viewed in the axial plane (Collin and Fritzsch 1993). In some specimens of *Euphanerops longaevus* the spherical aspect of the lateral plates is not totally present and the cone-shaped structure is observed (Figs. 2A–2C, and 4C). Along the growth series, for every 1% increase in the TL, the lateral plates length increases by about 0.9%. Our interpretation is then in favour of the preservation of eye lenses in *Euphanerops longaevus*.

In adult lampreys, the annular cartilage supports the buccal funnel and a pair of slender spine-like stylets articulate with this complex (Hardisty 1981) (Fig. 4A, ann. cart, st). The annular cartilage and the stylets develop simultaneously and relatively early during the larval stage in *Euphanerops longaevus* (Fig. 7). The labelling of those structures follows the identification in lamprey, however, this does not imply homologies between lamprey and *Euphanerops longaevus* skeletal elements. Another interpretation for the stylets could be the presence of displaced dorsal spines in *Euphanerops longaevus*, but the histological composition does not correspond to a dermal structure because of the presence of large chondrocyte vacuoles, whereas dermal spines are made of hydroxyapatite and lack a cartilaginous precursor during early ontogeny (Chevrinais et al. 2015*a*). Our new interpretation based on the anatomy of *Petromyzon marinus* allow us to specify that the element identified by Janvier and Arsenault (2007) as the "anterior ventral rod" and the "diffused mineralized matter" correspond to the left and right stylets, respectively.

Even in the smallest specimens of *Euphanerops longaevus*, paired brownish ovoid elements identified as "mineralized

matter in the otic region" by Janvier and Arsenault (2007) (Figs. 2A, 2B, and 2D) are present. A recent interpretation of similar elements emerges from van der Brugghen (2015) about the anaspid-like *Ciderius cooperi*, in which these elements are described as "parachordal elements", which are skeletal elements surrounding the notochord. These are likely homologous to notochordal cartilages found dorsally to the notochord in *Petromyzon marinus* and ventrally and dorsally to the notochord in *Euphanerops longaevus* (Chevrinais et al. 2018). However, the chemical composition recorded in *Euphanerops longaevus* does not agree with this hypothesis. These mineralized elements are also present in the Scottish species of Euphaneropidae (*Achanarella trewini* and *Cornovichthys blaauweni)* (Newman and Trewin 2001; Newman 2002) and are interpreted as otic capsules (van der Brugghen 2017). In the extant lamprey, *Lampetra planeri*, the otic capsules are in the posterior part of the neurocranium and are made of cartilage, but an amorphous otolith is also present, made of aggregates of numerous spherical otoconia composed of carbonate-rich fluorapatite (i.e., apatite) (Avallone et al. 2007). The position of lamprey otolith relative to the head is similar to that of jawed vertebrate otoliths or statoconia (Schultze 1990), and their microscale morphology recall the spherules present in *Euphanerops longaevus* (Lychakov 1995). Therefore, we interpret the mineralized matter in the otic region of *Euphanerops longaevus* as otoliths, similar in composition to lamprey otoliths. During the ontogeny in *Euphanerops longaevus*, these elements are present in larvae and juveniles but are difficult to observe in adults. Most likely these elements are not visible in an adult *Euphanerops longaevus* because of a progressive formation of the neurocranium covering these elements during ontogeny.

The structure of the branchial cartilage is similar between *Petromyzon marinus* (Fig. 4E) and *Euphanerops longaevus* (Fig. 3J), both of which have stacked chondrocytes. In addition, the topology of the branchial elements is also similar with the presence of epitrematic and hypotrematic bars and seven arches in adults (Figs. 4A and 4H). This similarity differs from Janvier et al. (2006), likely because they described the branchial apparatus in immature specimens. In MHNM 01-123 (Fig. 2E), ventral to the notochord, there are three different types of cartilaginous elements (Fig. 4G). First, the branchial apparatus shows seven arches with epitrematic and hypotrematic bars consisting of stacked chondrocytes (Fig. 4H). Second, more ventrally, a cartilaginous background without any particular topology with spherulitic cartilage and repeated rod shape structures resembling ribs is observed (Fig. 4H). Ventrally, radials, fin supports and meso-, meta-, and pterygium-like elements of the paired anteroventral fins are observed from the posterior extremity of the annular cartilage to the pelvic region (Chevrinais et al. 2018). In this context, the numerous structures originally interpreted as "gill-ray like mineralized rods" (Janvier and Arsenault 2007, fig. 25) could rather be numerous elements of the elongated anteroventral paired fins (supports) in adults. In the smallest specimens (larval and juvenile specimens), the branchial apparatus shows up to 30 vertical structures that could be interpreted as gill bars. However, those vertical structures are not preserved well enough for us to state that each structure represents an individual arch. If each structure represents an individual arch, the presence in smallest specimens of up to 30 gill bars in comparison with what we observe in adult specimens (up to seven bars) suggests either (1) a complete remodelling of the branchial region during ontogeny or (2) a taphonomic bias erroneously showing seven arches preserved in the adult or 30 gill bars in immature specimens. Even if the number of gill bars is higher in immatures than in adults, the relative proportion of the branchial basket remains constant as TL increases (for every 1% increase in TL, the branchial basket length increases by about 1%). If future studies reject the taphonomic bias hypothesis, this condition in *Euphanerops longaevus* differs from that in *Petromyzon marinus* in which the number of branchial arches is established early in the larval stage and remains unchanged through metamorphosis and the adult stage (Hardisty 1981).

Postcranial skeleton

Chevrinais et al. (2018) concluded that a few postcranial characters of *Euphanerops longaevus* (e.g., regionalization of the vertebral column, pelvic girdle, intromittent organ) occurred prior to the origin of jawed vertebrates, even though these features are generally considered as gnathostome synapomorphies.

One of the most important characters in the early evolutionary history of vertebrates is the presence of fins (Coates 1993; Wilson et al. 2007). Janvier and Arsenault (2007) did not recognize the presence of a dorsal fin in *Euphanerops longaevus*. They suggested the presence of "dorsal arcualia" where we identify dorsomedian rod elements and dorsal fin supports located dorsally to the notochord, above the dorsal arcualia (Fig. 5B). Among dorsal fin supports, some of them are bifurcating distally (Fig. 5B). However, in the other naked-anaspid taxa of the Escuminac Formation, the presence of a dorsal finfold has been proposed in *Endeiolepis aneri* (synonym *Euphanerops longaevus)* (Janvier 1996*a*) and the presence of dorsal fin elements has been suggested in *Legendrelepis parenti* (Arsenault and Janvier 1991). The dorsal fin of anaspids lacks endoskeletal elements; a dorsal row of scutes extending on the anterior half of the dorsal border has been observed in *Birkenia*, *Pterygolepis*, *Rhyncholepis*, *Pharyngolepis*, and *Lasanius* (Stensiö 1939; Wu et al. 2021). The presence of bifurcating fin elements made of cartilage in *Euphanerops longaevus*, similar to those in the dorsal fins observed in *Petromyzon marinus*, further give credence to the interpretation by Chevrinais et al. (2018) that the structures previously identified as dorsal arcualia indeed support a dorsal fin.

The anal fin in *Euphanerops longaevus* has been recognized for a long time; however, its paired condition is still debated (Janvier and Arsenault 2007; Sansom et al. 2013; Chevrinais et al. 2018). Because our study did not give any new evidence about the presence of a single or paired anal fin(s), we use the term "anal fin(s)" in *Euphanerops longaevus*. The anal fin is normally absent from *Petromyzon marinus,* but has been exceptionally reported in two female specimens of *Petromyzon marinus* (Vladykov 1973; Vladykov and Kott 1980); it may represent an atavistic expression of a plesiomorphic condition (Renaud 2011). The plesiomorphic condition being represented by the

presence of anal fin(s) in *Euphanerops longaevus* (Janvier and Arsenault 2007; Sansom et al. 2013), some other anaspids, and one thelodont (Larouche et al. 2019). In osteostracans, a horizontal caudal lobe has been identified but the homology with the anal fin is unclear (Sansom 2009).

Comparative ontogeny of *Petromyzon marinus* and *Euphanerops longaevus* reveals similarities in multiple systems: e.g., olfactory organ, eye lenses, annular cartilage, otoliths, branchial apparatus, dorsal fin. This information, added to the description by Chevrinais et al. (2018), supports a shared evolutionary history between lampreys and jawless fish belonging to Euphaneropidae. The evolutionary history of early vertebrates should be further investigated using morphological and developmental analyses that include all the species belonging to Euphaneropidae and new phylogenetic analyses of early vertebrates conducted.

Ackowledgements

We thank J. Kerr, O. Matton, and F. Charest (MHNM) and E. Bernard (NHMUK) for access to collections; C. Belzile (UQAR) and V. Roy (UQAR) for methodological help; D. Potvin-Leduc (UQAR), P. Janvier (MNHN), M.V.H. Wilson (U Alberta) and O. Larouche (UQAR) for helpful discussions and the two anonymous reviewers for constructive comments.

Article information

History dates

Received: 24 May 2022
Accepted: 2 December 2022
Version of record online: 16 January 2023

Copyright

Data availability

Data are available as supplementary material.

Author information

Author ORCIDs

Marion Chevrinais https://orcid.org/0000-0002-7305-0485

Author contributions

Conceptualization: MC, RC
Data curation: MC, CM
Formal analysis: MC, CM, CBR
Funding acquisition: CBR, RC
Investigation: MC, CM, RC
Methodology: MC, CM, CBR, RC
Supervision: CBR, RC
Visualization: MC, CM
Writing – original draft: MC, CM
Writing – review & editing: MC, CBR, RC

Competing interests

The authors declare that they have no competing financial interests.

Funding information

This research was supported by Natural Sciences and Engineering Research Council 238612 (to RC).

Supplementary material

Supplementary data are available with the article at https://doi.org/10.1139/CJES-2022-0062.

References

Arsenault, M., and Janvier, P. 1991. The anaspid-like craniates of the Escuminac Formation (Upper Devonian) from Miguasha (Quebec, Canada), with remarks on anaspid–petromyzontid relationships. *In* Early vertebrates and related problems of evolutionary biology. *Edited by* C. Mee-Man, L. Yu-hai and Z. Guo-rui. Science Press, Beijing, China. pp. 19–40.

Avallone, B., Fascio, U., Balsamo, G., Bianco, P.G., Balassone, G., and Marmo, F. 2007. Morphogenesis of otoliths during larval development in brook lamprey, *Lampetra planeri*. Italian Journal of Zoology, **74**(3): 247–258. doi:10.1080/11250000701459301.

Bardack, D., and Zangerl, R. 1971. Lampreys in the fossil record. *In* The biology of lampreys. *Edited by* M. Hardisty and I. Potter. Academic Press, London. pp.67–84.

Berio, F., Broyon, M., Enault, S., Pirot, N., López-Romero, F.A., and Debiais-Thibaud, M. 2021. Diversity and evolution of mineralized skeletal tissues in chondrichthyans. Frontiers in Ecology and Evolution, **9**: 660767. doi:10.3389/fevo.2021.660767.

Chevrinais, M., Balan, E., and Cloutier, R. 2015a. New insights in the ontogeny and taphonomy of the Devonian acanthodian *Triazeugacanthus affinis* from the Miguasha Fossil-Lagerstätte, Eastern Canada. Minerals, **6**(1): 1. doi:10.3390/min6010001.

Chevrinais, M., Cloutier, R., and Sire, J.-Y. 2015b. The revival of a so-called rotten fish: the ontogeny of the Devonian acanthodian Triazeugacanthus. Biology Letters, **11**(2): 20140950. doi:10.1098/rsbl.2014.0950. PMID: 25694507.

Chevrinais, M., Sire, J.-Y., and Cloutier, R. 2017. Unravelling the ontogeny of a Devonian early gnathostome, the "acanthodian" Triazeugacanthus affinis (eastern Canada). PeerJ, **5**: e3969. doi:10.7717/peerj.3969. PMID: 29094000.

Chevrinais, M., Johanson, Z., Trinajstic, K., Long, J., Morel, C., Renaud, C.B., and Cloutier, R. 2018. Evolution of vertebrate postcranial complexity: axial skeleton regionalization in paired appendages in a Devonian jawless fish. Palaeontology, **61**(6): 949–961. doi:10.5061/dryad.1r634nj.

Cloutier, R. 1996. The primitive actinistian Miguashaia bureaui Schultze (Sarcopterygii). *In* Devonian fishes and plants of Miguasha, Quebec, Canada. *Edited by* H.-P. Schultze and R. Cloutier. Verlag Dr Friedrich Pfeil. pp. 227–247.

Cloutier, R. 2010. The fossil record of fish ontogenies: insights into developmental patterns and processes. Seminars in Cell & Developmental Biology, **21**: 400–413.

Cloutier, R., Loboziak, S., Candilier, A-.M., and Blieck, B. 1996. Biostratigraphy of the Upper Devonian Escuminac Formation, eastern Québec, Canada: a comparative study based on miospores and fishes. Review of Palaeobotany and Palynology, **93**(1–4): 191–215. doi:10.1016/0034-6667(95)00126-3.

Cloutier, R., Proust, J.-N., and Tessier, B. 2011. The Miguasha Fossil-Fish-Lagerstätte: a consequence of the Devonian land-sea interactions. Palaeobiodiversity and Palaeoenvironments, **91**: 293–323. doi:10.1007/s12549-011-0058-0.

Coates, M.I. 1993. Actinopterygian and acanthodian fishes from the Viséan of East Kirkton, West Lothian, Scotland. Earth and Environmental Science Transactions of the Royal Society of Edinburgh, **84**(3–4): 317–327. doi:10.1017/S0263593300006131.

Collin, S.P., and Fritzsch, B. 1993. Observations on the shape of the lens in the eye of the silver lamprey, *Ichthyomyzon unicuspis*. Canadian Journal of Zoology, **71**(1): 34–41. doi:10.1139/z93-006.

Delfino, M., and Sánchez-Villagra, M.R. 2010. A survey of the rock record of reptilian ontogeny. Seminars in Cell & Developmental Biology, 432–440. Elsevier.

Dohrn, A. 1886. Studien zur urgeschichte des Wirbelthierkörpers IX. Die bedeutung der unpaaren flosse für die beurtheilung der genealogischen Stellung der Tunicaten und des Amphioxus, und die reste der Beckenflosse bei Petromyzon. Mittheilungen aus der Zoologischen Station Neapel, **6**. 399–480.

Donoghue, P.C.J., and Sansom, I.J. 2002. Origin and early evolution of vertebrate skeletonization. Microscopy Research and Technique, **59**(5): 352–372. doi:10.1002/jemt.10217. PMID: 12430166.

Fischer-Rousseau, L., Cloutier, R., and Zelditch, M.L. 2009. Morphological integration and developmental progress during fish ontogeny in two contrasting habitats. Evolution & Development, **11**(6): 740–753.

Forey, P.L. 1984. Yet more reflections on agnathan–gnathostome relationships. Journal of Vertebrate Paleontology, **4**(3): 330–343. doi:10.1080/02724634.1984.10012013.

Fröbisch, N.B., Olori, J.C., Schoch, R.R., and Witzmann, F. 2010. Amphibian development in the fossil record. Seminars in Cell & Developmental Biology, 424–431. Elsevier.

Gabbott, S.E., Donoghue, P.C.J., Sansom, R.S., Vinther, J., Dolocan, A., and Purnell, M.A. 2016. Pigmented anatomy in carboniferous cyclostomes and the evolution of the vertebrate eye. Proceedings of the Royal Society B, **283**(1836): 20161151. doi:10.1098/rspb.2016.1151.

Gagnier, P.-Y. 1996. Acanthodii. *In* Devonian fishes and plants of Miguasha, Quebec, Canada. *Edited by* H.-P. Schultze and R. Cloutier. Verlag Dr. Friedrich Pfeil, München. pp. 149–164.

Graham-Smith, W. 1935. *Scaumenella mesacanthi*, gen. et sp. n., a peculiar organism from the Upper Devonian of Scaumenac Bay, P.Q., Canada. Annals and Magazine of Natural History, **16**(10): 473–476. doi:10.1080/00222933508655072.

Green, S.A., and Bronner, M.E. 2014. The lamprey: a jawless vertebrate model system for examining origin of the neural crest and other vertebrate traits. Differentiation, **87**(1–2): 44–51. doi:10.1016/j.diff.2014.02.001. PMID: 24560767.

Green, W.W., Boyes, K., McFadden, C., Daghfous, G., Auclair, F., Zhang, H., et al. 2017. Odorant organization in the olfactory bulb of the sea lamprey. Journal of Experimental Biology, **220**(7): 1350–1359. PMID: 28183864.

Grogan, E.D., and Lund, R. 2000. *Debeerius ellefseni* (fam. nov., gen. nov., spec. nov.), an autodiastylic chondrichthyan from the Mississippian Bear Gulch Limestone of Montana (USA), the relationships of the chondrichthyes, and comments on gnathostome evolution. Journal of Morphology, **243**(3): 219–245. doi:10.1002/(SICI).1097-4687.(200003).243:3⟨219::AID-JMOR1⟩3.0.CO;2-1. PMID: 10681469.

Grünbaum, T., Cloutier, R., and Vincent, B. 2012. Dynamic skeletogenesis in fishes: insight of exercise training on developmental plasticity. Developmental Dynamics, **241**(10): 1507–1524. doi:10.1002/dvdy.23837. PMID: 22821586.

Hardisty, M. 1979. Ecology and behavior. *In* Biology of the cyclostomes. *Edited by* M.W. Hardisty. Chapman and Hall. pp. 51–75.

Hardisty, M.W. 1981. The skeleton. *In* The biology of lampreys. *Edited by* M.W. Hardisty and I.C. Potter. Academic Press, London. pp. 333–372.

Hardisty, M.W. 1982. Lampreys and hagfishes: analysis of cyclostome relationships. *Edited by* M.W. Hardisty and I. Potter. Academic Press, London.

Heimberg, A.M., Cowper-Sal·lari, R., Sémon, M., Donoghue, P.C.J., and Peterson, K.J. 2010. MicroRNAs reveal the interrelationships of hagfish, lampreys, and gnathostomes and the nature of the ancestral vertebrate. Proceedings of the National Academy of Sciences of the United States of America, **107**(45): 19379–19383. doi:10.1073/pnas.1010350107.

Janvier, P. 1981. The phylogeny of the Craniata, with particular reference to the significance of fossil "agnathans. Journal of Vertebrate Paleontology, **1**(2): 121–159. doi:10.1080/02724634.1981.10011886.

Janvier, P. 1996a. Early vertebrates. Oxford University Press, United States.

Janvier, P. 1996b. The dawn of the vertebrates: characters versus common ascent in the rise of current vertebrate phylogenies. Palaeontology, **39**(2): 259–287.

Janvier, P. 1996c. The Miguasha "Anaspida". *In* Devonian fishes and plants of Miguasha, Quebec, Canada. *Edited by* H.-P. Schultze and R. Cloutier. Verlag Dr. Friedrich Pfeil, München. pp.134–140.

Janvier, P. 2010. MicroRNAs revive old views about jawless vertebrate divergence and evolution. Proceedings of the National Academy of Sciences of the United States of America, **107**(45): 19137–19138. doi:10.1073/pnas.1014583107.

Janvier, P., and Arsenault, M. 2007. The anatomy of *Euphanerops longaevus* Woodward, 1900, an anaspid-like jawless vertebrate from the Upper Devonian of Miguasha, Quebec, Canada. Geodiversitas, **29**(1): 143–216.

Janvier, P., Desbiens, S., Willett, J.A., and Arsenault, M. 2006. Lamprey-like gills in a gnathostome-related Devonian jawless vertebrate. Nature, **440**(7088): 1183–1185. Available from http://www.nature.com/nature/journal/v440/n7088/suppinfo/nature04471_S1.html [accessed Mar 16 2022]. PMID: 16641994.

Johanson, Z., and Trinajstic, K. 2014. Fossilized ontogenies: the contribution of placoderm ontogeny to our understanding of the evolution of early gnathostomes. Palaeontology, **57**: 505. doi:10.1111/pala.12093.

Larouche, O., Zelditch, M.L., and Cloutier, R. 2019. A critical appraisal of appendage disparity and homology in fishes. Fish and Fisheries, **20**(6): 1138–1175. doi:10.1111/faf.12402.

Lehman, J.-P. 1957. Un problème non résolu: l'origine des vertébrés. La Nature (Science, progrès, découverte), **85**: 174–177.

Lindgren, J., Uvdal, P., Sjövall, P., Nilsson, D.E., Engdahl, A., Schultz, B.P., and Thiel, V. 2012. Molecular preservation of the pigment melanin in fossil melanosomes. Nature Communications, **3**: 824. doi:10.1038/ncomms1819. PMID: 22569368.

Lychakov, D.V. 1995. Study on structure of the otolith membrane in the lamprey *Lampetra fluviatilis* in the context of otolith and otoconium evolution. Journal of Evolutionary Biochemistry and Physiology, **31**(2): 90–97.

Maisey, J.G. 1986. Heads and tails: a chordate phylogeny. Cladistics, **2**(4): 201–256. doi:10.1111/j.1096-0031.1986.tb00462.x. PMID: 34949070.

Martin, W.M., Bumm, L.A., and McCauley, D.W. 2009. Development of the viscerocranial skeleton during embryogenesis of the sea lamprey, *Petromyzon marinus*. Developmental Dynamics, **238**(12): 3126–3138. doi:10.1002/dvdy.22164. PMID: 19924811.

Miyashita, T., Coates, M.I., Farrar, R., Larson, P., Manning, P.L., and Wogelius, R.A. 2019a. Hagfish from the Cretaceous Tethys Sea and a reconciliation of the morphological–molecular conflict in early vertebrate phylogeny. Proceedings of the National Academy of Sciences of the United States of America, **116**(6): 2146–2151. doi:10.1073/pnas.1814794116.

Miyashita, T., Green, S.A., and Bronner, M.E. 2019b. Comparative development of cyclostomes. Evolution and Development of Fishes, 30–58.

Miyashita, T., Gess, R.W., Tietjen, K., and Coates, M.I. 2021. Non-ammocoete larvae of palaeozoic stem lampreys. Nature, **591**(7850): 408–412. doi:10.1038/s41586-021-03305-9. PMID: 33692547.

Newman, M.J. 2002. A new naked jawless vertebrate from the middle Devonian of Scotland. Palaeontology, **45**(5): 933–941. doi:10.1111/1475-4983.00269.

Newman, M.J., and Trewin, N.H. 2001. A new jawless vertebrate from the middle Devonian of Scotland. Palaeontology, **44**(1): 43–51. doi:10.1111/1475-4983.00168.

Piveteau, J., Lehman, J.-P., and Dechaseaux, C. 1978. Précis de paléontologie des vertébrés. *Edited by* M. Hungary.

R Core Team. 2022. R: a language and environment for statistical computing. R Foundation for Statistical Computing, Vienna, Austria.

Renaud, C.B. 2011. Lampreys of the world. In An annotated and illustrated catalogue of lamprey species known to date. Food and Agriculture Organization of the United Nations Species Catalogue for Fisheries. pp. 5.

Ritchie, A. 1968. New evidence on *Jamoytius kerwoodi* White, an important ostracoderm from the Silurian of Lanarkshire, Scotland. Palaeontology, **11**(1): 21–39.

Sánchez-Villagra, M.R. 2010. Developmental palaeontology in synapsids: the fossil record of ontogeny in mammals and their closest relatives. Proceedings of the Royal Society, **277**(1685): 1139–1147. doi:10.1098/rspb.2009.2005.

Sansom, R.S. 2009. Phylogeny, classification and character polarity of the Osteostraci (Vertebrata). Journal of Systematic Palaeontology, **7**(1): 95–115. doi:10.1017/S1477201908002551.

Sansom, R.S., Gabbott, S.E., and Purnell, M.A. 2013. Unusual anal fin in a Devonian jawless vertebrate reveals complex origins of paired appendages. Biology Letters, **9**(3): 20130002. doi:10.1098/rsbl.2013.0002. PMID: 23576777.

Schultze, H.-P. 1984. Juvenile specimens of *Eusthenopteron foordi* Whiteaves, 1881 (*Osteolepiform rhipidistian*, Pisces) from the late Devonian of Miguasha, Quebec, Canada. Journal of Vertebrate Paleontology, **4**(1): 1–16. Available from http://www.jstor.org/stable/4522961 [accessed Feb 23 2022]. doi:10.1080/02724634.1984.10011982.

Schultze, H.-P. 1990. A new acanthodian from the Pennsylvanian of Utah, U.S.A., and the distribution of otoliths in gnathostomes. Journal of Vertebrate Paleontology, **10**(1): 49–58. doi:10.1080/02724634.1990.10011789.

Shimeld, S.M., and Donoghue, P.C.J. 2012. Evolutionary crossroads in developmental biology: cyclostomes (lamprey and hagfish). Development (Cambridge), **139**(12): 2091–2099. doi:10.1242/dev.074716. PMID: 22619386.

Stensiö, E.A. 1939. A new anaspid from the Upper Devonian of Scaumenac bay in Canada, with remarks on the other anaspids. Kungl. Svenska Vetenskapsakademiens Handlingar, **3**(18): 3–25.

Tarlo, L.B. 1960. The invertebrate origins of the vertebrates. International Geological Congress. Edited by T. Sorgenfrei. Copenhagen. pp. 113–123.

Tretjakoff, D. 1926. Die Wirbelsäule des Neunauges. Anatomischer Anzeiger, **61**: 387–396.

Van Denbossche, J., Youson, J.H., Pohlman, D., Wong, E., and Zielinski, B.S. 1997. Metamorphosis of the olfactory organ of the sea lamprey (*Petromyzon marinus* L.): morphological changes and morphometric analysis. Journal of Morphology, **231**(1): 41–52. doi:10.1002/(SICI)1097-4687(199701)231:1%3c41::AID-JMOR4%3e3.0.CO;2-R. PMID: 29852668.

van der Brugghen, G. 2015. *Ciderius cooperi* gen. nov., sp. nov., the earliest known euphaneropid from the Lower Silurian of Scotland. Netherlands Journal of Geosciences, **94**: 279–288. doi:10.1017/njg.2015.18.

van der Brugghen, G. 2017. Taphonomy versus taxonomy and the synonyms of *Euphanerops longaevus* Woodward, 1900 (Agnatha) occurring at the middle Devonian Achanarras Quarry of Caithness, Scotland. Neues Jahrbuch für Geologie und Paläontologie, **286**(3): 329–347. doi:10.1127/njgpa/2017/0701.

Vladykov, V.D. 1973. A female sea lamprey (*Petromyzon marinus*) with a true anal fin, and the question of the presence of an anal fin in Petromyzonidae. Canadian Journal of Zoology, **51**(2): 221–224. doi:10.1139/z73-032.

Vladykov, V.D., and Kott, E. 1980. Description and key to metamorphosed specimens and ammocoetes of Petromyzonidae found in the Great Lakes region. Canadian Journal of Fisheries and Aquatic Sciences, **37**(11): 1616–1625. doi:10.1139/f80-208.

Wilson, M.V.H., Hanke, G.F., and Märss, T. 2007. Paired fins and jawless vertebrates and their homologies across the "agnathan–gnathostome" transition. *In* Major transitions in vertebrate evolution. *Edited by* J.S. Anderson and H.-D. Sues. Indiana University Press, USA. pp.122–149.

Woodward, A.S. 1900. On a new Ostracoderm (Euphanerops longaevus) from the Upper Devonian of Scaumenac Bay, Province of Quebec, Canada. Annals and Magazine of Natural History, **5**(5): 416–419. doi:10.1080/00222930008678308.

Wu, F., Chang, M.-M., and Janvier, P. 2021. A new look at the cretaceous lamprey Mesomyzon Chang, Zhang & Miao, 2006 from the Jehol Biota. Geodiversitas, **43**(23): 1293–1307.